Title No. 120-S84

# Design of Glass Fiber-Reinforced Polymer-Reinforced Concrete Columns per ACI CODE-440.11-22

by Zahid Hussain and Antonio Nanni

This paper is an attempt at a better understanding of design provisions of ACI CODE-440.11-22, building code for the design of glass fiber-reinforced polymer (GFRP)-reinforced concrete (RC) columns. Sway and a non-sway column examples originally designed with steel reinforcement were redesigned using GFRP longitudinal bars and ties as per provisions of ACI CODE-440.11-22 to analyze the effect of changing reinforcement type. Columns were designed with both low-modulus ( $E_f = 6500 \text{ ksi}$ ), and high-modulus ( $E_f = 8700 \text{ ksi}$ ) GFRP bars. A parametric study was carried out by varying the concrete compressive strength, the cross-section aspect ratio, and the resultant load eccentricity. GFRP-RC columns require larger cross-section dimensions and more reinforcement area than steel-RC columns irrespective of the GFRP elastic modulus when subjected to the same demand. The concrete strength has a significant effect on the dimensions of GFRP-RC columns, and rectangular sections were found to be more efficient than square sections with the same gross concrete area in the presence of moment. GFRP-RC columns subject to high eccentricity loads take advantage of GFRP tensile properties and, thus, are more efficient.

**Keywords:** building code; concrete columns; eccentricity; glass fiber-reinforced polymer (GFRP) reinforcement.

#### INTRODUCTION

Fiber-reinforced polymer (FRP) bars, being a competitive option for reinforced concrete (RC) members in aggressive environments, were not allowed in compression members in the previous editions of the ACI 440 Guide. The primary reason for this exclusion was a lack of information regarding the behavior of FRP-RC members subjected to compressive loads. However, researchers have been actively investigating the behavior of glass FRP (GFRP)-RC columns during the last decade and have found GFRP-RC columns to be permissible structural elements. In fact, several experimental studies investigated the effect of the compressive behavior of longitudinal GFRP bars by testing RC columns<sup>2-5</sup> with an overall positive assessment of their feasibility. Jawaheri Zadeh and Nanni<sup>6</sup> provided information on flexural stiffness in frame analysis for GFRP-RC that resulted in close correspondence to limits proposed by Bischoff.<sup>7</sup> Similarly, Hadhood et al., among other researchers, proposed a 1% minimum reinforcement necessary to maintain section integrity to achieve a nominal capacity of columns. Khorramian and Sadeghian<sup>10</sup> performed structural tests validating the performance of GFRP-RC columns with reinforcement ratios as high as 5.3%. Given, these significant advances in research over the past decade, the new ACI CODE-440.11-22 Building Code<sup>11</sup> permits the use of GFRP-RC columns with limitations to non-seismic zones and structures not requiring fire resistance. The addition of provisions for compressive members is a critical development for practitioners interested in nonmetallic reinforcement as it allows designing and construction of a building entirely with GFRP-RC.

Though ACI CODE-440.11-22 permits the design of columns using GFRP bars, due to their lower reliability, the minimum compressive strength properties of GFRP bars are not specified in ASTM D7957. 12 As stipulated in ACI CODE-440.11-22, in pure compression, their presence can be treated as having the same stiffness and strength as those of the surrounding concrete. However, in the presence of moment, GFRP reinforcement may effectively contribute to the column capacity. Therefore, this study is carried out to show the implications of current Code provisions on the design of GFRP-RC compressive members.

#### **RESEARCH SIGNIFICANCE**

The recently published ACI CODE-440.11-22<sup>11</sup> allows the design of columns with GFRP reinforcement. Due to remaining knowledge gaps in the behavior of GFRP-RC columns, some Code provisions were only analytically developed and verified by incorporating differences in material properties with steel-RC. This study shows the implications of Code provisions and highlights the areas for further research.

#### **METHODOLOGY**

In this study, a column part of a sway frame from the ACI Reinforced Concrete Design Handbook, <sup>13</sup> a Companion to ACI 318-19, <sup>14</sup> is selected and redesigned using GFRP reinforcement. This column is part of an interior, continuous, six-bay frame, and built integrally with a 7 in. (178 mm) deep slab, as shown in Fig. 1(a). The constituent materials selected for column design are listed in Table 1. The concrete strength  $f_c$ ' is 5000 psi (35 MPa), while the GFRP type is compliant with material specification based on ASTM D7957. <sup>12</sup> For the non-sway case, a column from a frame part of an industrial building was taken from the textbook by Wight and Macgregor, <sup>15</sup> as shown in Fig. 1(b). This is a laterally braced column with a beam on one side, as shown in Fig. 1(b). The concrete strength  $f_c$ ' for this column was 4000 psi (28 MPa) (as given in the textbook), while

ACI Structural Journal, V. 120, No. 5, September 2023.

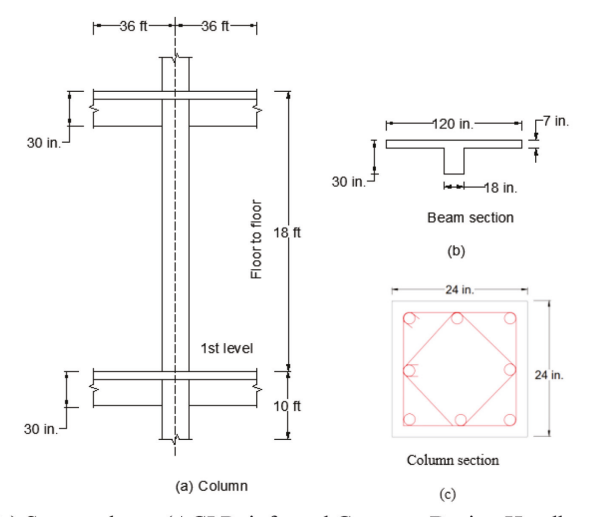
MS No. S-2022-307.R3, doi: 10.14359/51738838, received April 10, 2023, and reviewed under Institute publication policies. Copyright © 2023, American Concrete Institute. All rights reserved, including the making of copies unless permission is obtained from the copyright proprietors. Pertinent discussion including author's closure, if any, will be published ten months from this journal's date if the discussion is received within four months of the paper's print publication.

Table 1—Properties of GFRP reinforcement and concrete

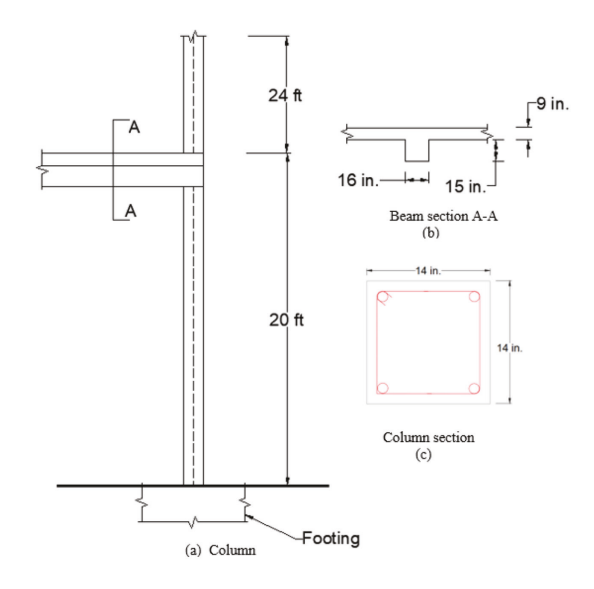
	Nominal		Elastic	Guaranteed tensile	Ultimate	Concrete		
Designation	diameter, in.	Nominal area, in. <sup>2</sup>			strain, %	Sway column	Non-sway column	Clear cover, in.
GFRP-4	0.5	0.2		108	0.016			1.5
GFRP-8	1.0	0.79	6500	84.5	0.013		4000	
GFRP-9	1.128	1.0		82	0.013	5000		
GFRP-4*	0.5	0.2		139.5	0.016	3000		
GFRP-8*	1.0	0.79	8700	120	0.013			
GFRP-9*	1.128	1.0		115	0.013			

<sup>\*</sup>New-generation GFRP bars with higher modulus of elasticity and guaranteed strength as proposed in an ASTM material spec under development.

Note: GFRP-4 = M13; GFRP-8 = M25; GFRP-9 = M29; 1 in. = 25.4 mm; 1 in.<sup>2</sup> = 645 mm<sup>2</sup>; 1 ksi = 6.89 MPa.



(a) Sway column (ACI Reinforced Concrete Design Handbook)<sup>13</sup>



(b) Non-sway column (Textbook by Wight and Macgregor)<sup>15</sup>

Fig. 1—Geometrical dimensions for: (a) sway column; and (b) non-sway column.

the GFRP has the same properties as for the sway column. Given that a new ASTM material specification is under development for a class of GFRP bars with higher modulus of elasticity and strength, this class of GFRP bars was also

Table 2—Strength reduction factor  $\Phi$  for moment, axial force, or combined moment and axial force (ACI CODE-440.11-22, Section 21.2.2)

Net tensile strain at failure in outermost layer of GFRP reinforcement $\epsilon_f$	Classification	Φ
$\varepsilon_f = \varepsilon_{fit}$	Tension-controlled	0.55
$\varepsilon_{fu} > \varepsilon_f > 0.8 \varepsilon_{fu}$	Transition	1.05 to 0.5 $\epsilon_f/\epsilon_{fu}$
$\varepsilon_f \leq 0.8 \varepsilon_{fu}$	Compression- controlled	0.65

considered. This study uses No. 8 and 9 (M25 and M29) nominal bar sizes for longitudinal reinforcement and No. 4 (M13) for stirrups/ties in all columns. The mechanical properties of GFRP bars in tension affecting design are listed in Table 1 and include guaranteed ultimate tensile strength  $f_{fit}$ , corresponding ultimate strain  $\varepsilon_{fit}$ , and modulus of elasticity  $E_f$ . GFRP compressive properties (that is, strength and stiffness) are not provided because, in design, the area of longitudinal GFRP bars in compression is considered equivalent to concrete.

#### **COLUMN PROVISIONS IN ACI CODE-440.11-22**

For applicable factored load combinations, design strength at all sections shall satisfy the requirements of ACI CODE-440.11-22, Section 10.5.1.1, given as follows

$$\Phi S_n \ge U \tag{1}$$

where  $S_n$  is nominal moment, shear, axial, or torsional strength; U is strength of a member or cross section required to resist factored loads; and  $\Phi$  is strength reduction factor as per ACI 440.11-22 and given in Table 2.

Because GFRP compression reinforcement will not contribute to the compression capacity of the cross section, the strength of a column subject to pure axial load is calculated using the gross concrete area and  $f_c$ , while treating GFRP as if it were concrete, as given in the Code Section 22.4.2.2

$$P_o = 0.85 f_c' A_g \tag{2}$$

where  $P_o$  is nominal axial strength at zero eccentricity.

The design tensile strain and strength of GFRP bar, in this study, were used as provided in Code Section 10.3.2.1, given as follows

If 
$$P_u > 0.10 f_c' A_g$$

Then, the limit on tensile strain is

$$\varepsilon_f = 0.01$$

Also,

Design strength = 
$$\min \begin{pmatrix} f_{fu} \\ 0.01 E_f \end{pmatrix}$$

Code Section 10.6.1 specifies a minimum reinforcement of 1% of the gross concrete area ( $A_g$ ) to provide resistance to bending and possibly concrete creep. Similarly, maximum reinforcement of 8% is specified to avoid congestion of reinforcing bars and to ensure that concrete can be properly consolidated.

The minimum number of bars is indicated by the Code Section 10.7.3, given as

Minimum number of longitudinal bars =

Rectangular or circular ties
 Triangular ties
 Enclosed by spirals

For longitudinal reinforcement, the minimum clear spacing between bars is specified in the Code Section 25.2.3 as follows

Minimum spacing between bars = 
$$\max\begin{pmatrix} 1.5 \text{ in.}(38 \text{ mm}) \\ 1.5d_b \\ 4/3d_{agg} \end{pmatrix}$$

where  $d_b$  is diameter of the longitudinal bar; and  $d_{agg}$  is diameter of the aggregate.

Code Section 25.7.2.3 states that every corner or alternate bar shall have lateral support by the corner of a tie with an included angle of not more than 135 degrees. Also, every bar shall have less than 6 in. (152 mm) clear on each side along the tie from a laterally supported bar.

The column size may be found from Eq. (2) by introducing a strength reduction factor; however, the values obtained in this study were significantly lower than those required by GFRP-RC columns. The stricter limits on slenderness for GFRP-RC columns will usually require bigger size columns. Authors, by trial and error, found following relations to give good approximation for an initial estimate for the size of a square column

Sway columns: 
$$A_g = \frac{P_u}{0.25 f_c'}$$

Non-sway columns: 
$$A_g = \frac{P_u}{0.15f_c'}$$

ACI CODE-440.11-22 provides three conditions to determine if the frame can be considered non-sway—namely, Code Sections 6.2.5, 6.6.4.3(a), and 6.6.4.3(b), listed as follows:

- 1. 6.2.5 states that, if the stiffness of bracing elements exceeds 12 times the gross lateral stiffness of the columns in the direction considered, a column in that story can be considered as non-sway.
- 2. 6.6.4.3 implies analyzing the columns as non-sway if condition (a) or (b) is satisfied:
- (a) The increase in column end moments due to secondorder effects does not exceed 5% of the first-order end moments.
- (b) The stability index does not exceed 0.05. The stability index for a given story, Q, shall be calculated as shown

$$Q = \frac{\sum P_u \delta_o}{V_{us} l_c} \tag{3}$$

where  $\sum P_u$  is total factored vertical load;  $V_{us}$  is horizontal story shear;  $\delta_o$  is first-order relative lateral displacement between the top and bottom of that story; and  $l_c$  is height of the column from the center to center of the joints.

GFRP-RC columns are more susceptible to the slenderness effects than steel-RC due to the lower stiffness of GFRP reinforcement compared to steel bars; therefore, more strict limits are imposed when checking slenderness effects for GFRP-RC columns. Slenderness effects can be neglected in both sway and non-sway frames if the following conditions of Code Sections 6.2.5.1(a) or 6.2.5.1(b) are satisfied, given herein as Eq. (4a), (4b), and (4c)

(a) For columns not braced against sidesway

$$\frac{kl_u}{r} \le 17 \tag{4a}$$

(b) For columns braced against sidesway

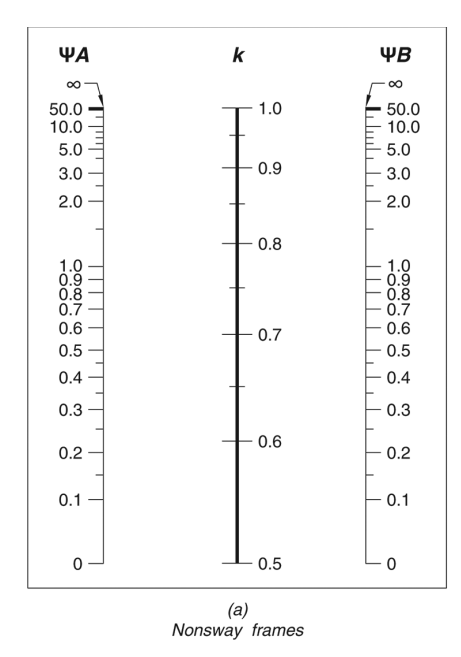
$$\frac{k l_u}{r} \le 29 + 12 \frac{M_1}{M_2}$$
 (4b)

$$\frac{kl_u}{r} \le 35 \tag{4c}$$

where  $M_1/M_2$  is negative if the column is bent in single curvature and positive for double curvature;  $l_u$  is unsupported length of column; and k is effective length factor for compression members. The effective length factor reflects column-end restraint conditions, which depend on the relative stiffness of the columns to the floor members at the top and bottom of joints given by

$$\omega = \frac{\left(\frac{EI}{l_c}\right)_{col,above} + \left(\frac{EI}{l_c}\right)_{col,below}}{\left(\frac{EI}{l}\right)_{beam,left} + \left(\frac{EI}{l}\right)_{beam,right}}$$
(5)

The values obtained by Eq. (5) are used to calculate k, using Fig. R6.2.5.1a and Fig. R6.2.5.1b for non-sway and sway frames, respectively, shown as Fig. 2, which is then



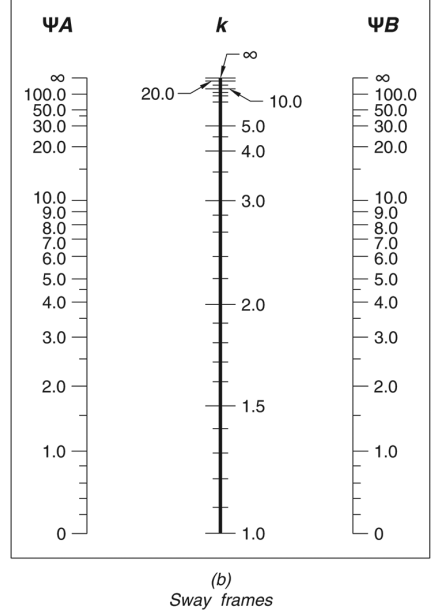


Fig. 2—Jackson and Moreland alignment charts (as given in ACI CODE-440.11-22).

used in Eq. 6.2.5.1a (4a), 6.2.5.1b (4b), and 6.2.5.1c (4c) to determine if the slenderness of columns could be neglected.

r is the radius of gyration. Its value can be calculated as given in Code Section 6.2.5.2

$$\sqrt{I_g/A_g}$$

which is (a) 0.30 times the dimension in the direction stability being considered for rectangular columns; or (b) 0.25 times the diameter of circular columns.

The moment of inertia and cross-sectional areas for elastic analysis at factored load level may be calculated by Code Section 6.6.3.1.1 and is shown in Table 3. It should be noted that moment of inertia values in ACI CODE-440.11-22 are lower than those provided in ACI 318-19 for steel-RC due to lower stiffness of GFRP reinforcement.

Code Section 6.6.4.6.4 requires magnifying the first-order moment to consider the second-order effects produced by slenderness in sway frames, given as Eq. (6a) and (6b)

$$M_1 = M_{1ns} + \delta_s M_{1s} \tag{6a}$$

$$M_2 = M_{2ns} + \delta_s M_{2s} \tag{6b}$$

where  $M_1$  is the lesser factored end moment on a compression member;  $M_{1ns}$  is the factored end moment on a compression member at the end at which  $M_1$  acts, due to loads that cause no appreciable sidesway, calculated using a first-order elastic frame analysis;  $M_{1s}$  is the factored end moment on a compression member at the end at which  $M_1$  acts, due to loads that cause appreciable sidesway, calculated using a first-order elastic frame analysis; and  $M_2$  is the greater factored end moment (always positive) on a compression member. If transverse loading occurs between supports,  $M_2$  is taken as the largest moment occurring on a member;  $M_{2ns}$  is the factored end moment on a compression member at the end at which  $M_2$  acts, due to loads that cause no appreciable

Table 3—Moment of inertia and cross-sectional area for elastic analysis

Member 6	end condition	Moment of inertia	Cross-sectional area for axial deformations	Cross-sectional area for shear deformations		
Со	lumns	$0.4I_g$				
W7-11-	Uncracked	$0.4I_g$	1.04	$b_w \ge h$		
Walls	Cracked	$0.15I_{g}$	$1.0A_g$			
В	eams	$0.15I_{g}$				

sidesway, calculated using a first-order frame analysis;  $M_{2s}$  is the factored end moment on a compression member at the end at which  $M_2$  acts, due to loads that cause appreciable sidesway, calculated using a first order elastic frame analysis; and  $\delta_s$  is the moment magnification factor for sway frames. Code Section 6.6.4.6.2 provides two ways to calculate its value, given as Eq. (7a) and (7b)

$$\delta_s = \frac{1}{1 - O} \ge 1 \tag{7a}$$

$$\delta_s = \frac{1}{1 - \frac{\sum P_u}{0.75 \sum P_c}} \ge 1 \tag{7b}$$

The critical buckling load  $P_c$  is calculated by Code Section 6.6.4.4.2, given as

$$P_c = \frac{\pi^2 (EI)_{eff}}{(kl_v)^2} \tag{8}$$

where  $P_c$  is critical buckling load;  $kl_u$  is effective length (the

length of a pin-ended column having same buckling load as original column); and  $(EI)_{eff}$  is effective moment of inertia, which can be calculated by Code Section 6.6.4.4.4a and 6.6.4.4.4b, given herein as Eq. (9a) and (9b)

$$(EI)_{eff} = \frac{0.24 E_c I_g}{1 + B_{dns}}$$
 (9a)

$$(EI)_{eff} = \frac{0.2E_c I_g}{1 + B_{dns}} + 0.75 E_f I_f$$
 (9b)

where  $B_{dns}$  is the ratio of maximum factored sustained axial load to maximum factored axial load; and  $I_f$  is the moment of inertia of the GFRP bars about the centroid of the cross section.

Code Section 6.6.4.5 implies amplifying  $M_2$  for the effects of member curvature in a non-sway frame given as

$$M_c = \delta M_2 \tag{10}$$

where  $M_c$  is factored moment amplified for the effects of member curvature; and  $\delta$  is magnification factor for non-sway frames as given in Code Section 6.6.4.5.2

$$\delta = \frac{C_m}{1 - \frac{P_u}{0.75P_c}} \ge 1.0 \tag{11}$$

where  $C_m$  (factor relating actual moment diagram to an equivalent uniform moment diagram) shall be in accordance with 6.6.4.5.3a and 6.6.4.5.3b, given herein as Eq. (12a) and (12b):

(a) For columns without transverse loads applied between supports

$$C_m = 0.6 - 0.4 \frac{M_1}{M_2} \tag{12a}$$

(b) For columns with transverse loads applied between supports

$$C_m = 1.0 \tag{12b}$$

# EXAMPLES OF COLUMN DESIGN AND DISCUSSION

The required strength for the two columns subjected to lateral and gravity loads was checked using the factored load combinations in Chapter 5 and analysis procedures in Chapter 6 of the ACI CODE-440.11. The calculated values of axial load, moment, and shear demands used in this study are given in Table 4 as originally available from the sources of the steel-RC cases. <sup>12,15</sup> It should be noted that for simplicity, a single combination of ultimate axial load and moment (that is,  $P_u$  and  $M_u$ ) for each of the two columns was adopted, whereas in practice, the demand of several combinations of loads and moments must be satisfied. Also, the design was carried out by keeping the reinforcement amount as close as possible to the minimum requirements of the Code (that is,  $1\%A_p$ ).

# Sway column using low- and high-modulus GFRP bars

The column was designed using the Code-referenced low-modulus ( $E_f$ = 6500 ksi [44,815 MPa]) GFRP bars, with a concrete strength of 5000 psi (35 MPa). The columns were designed as per procedure provided in ACI CODE-440.11-22, Fig. R6.2.5.3. The column in this design example is

Table 4—Factored axial, shear, and moment values

Ultimate loads	Sway column	Non-sway column		
$V_u$ , kip	22	_		
$P_u$ , kip	789	134		
$(M_u)_{top}$ , kip-ft	145	38		
$(M_u)_{bott}$ , kip-ft	197	94.4		

Note: 1 kip = 4.44 kN; 1 kip-ft = 1.35 kN-m.

laterally unbraced; therefore, slenderness effects were checked as per ACI CODE-440.11-22, Eq. (6.2.5.1a) (that is,  $kl_{\nu}/r < 17$ ). The unsupported length of the column, as shown in Fig. 1(a), is 15.5 ft (4.72 m) and its cross-section dimensions were calculated using relations provided in this paper equal to 26 x 26 in. (660 x 660 mm). The effective length factor was calculated using alignment charts given in Fig. R6.2.5.1 in ACI CODE-440.11-22 (that is, Fig. 2), which depend on the relative stiffnesses of columns to the floor members at column top and bottom joints. In this design example, the column frames into beams at the top joint, whereas it frames at bottom in a two-way slab. It was assumed that the columns in the stories above and below had the same cross-section dimensions. The gross moment of inertia of the column was equal to 38,080 in.  $^4$  (15.8 × 10 $^9$ mm<sup>4</sup>), and the effective moment of inertia calculated as per Table 3 was equal to 15,232 in.  $^4$  (6.3 × 10  $^9$  mm $^4$ ).

As stated in ACI CODE-440.11-22, Section R6.6.3.1.1, it is sufficiently accurate to take the gross moment of inertia of a T-beam equal to twice that of its web. Using this approach, the moment of inertia of T-beams framing into the column at the top joint was calculated equal to 81,000 in.<sup>4</sup> (33.7 ×  $10^9 \text{ mm}^4$ ), and the effective moment of inertia as per Table 3 was equal to 12,150 in.<sup>4</sup> (5 ×  $10^9 \text{ mm}^4$ ). Similarly, the moment of inertia at the lower joint was calculated for the slab framing into the column. The width of the slab in the transverse direction was considered equal to 14 ft (4.3 m) and its thickness equal to 7 in. (178 mm), as given in the ACI 318-19 Design Handbook.<sup>13</sup> Its gross moment of inertia was calculated equal to 4802 in.<sup>4</sup> (2 ×  $10^9 \text{ mm}^4$ ), which reduced to 720 in.<sup>4</sup> (0.3 ×  $10^9 \text{ mm}^4$ ) when calculating effective moment of inertia as per Table 3.

The relative stiffness at the top and bottom joints was calculated as per Eq. (5) of this paper (as given in ACI CODE-440.11-22), which were found equal to 3 for top and 30 for bottom joints, respectively. Using relative stiffness factors in alignment charts given in Fig. 2, the effective length factor was calculated equal to 2.8 and radius of gyration equal to 7.5 from ACI CODE-440.11-22, Section 6.2.5.2. The values of effective length factor, unsupported length of column, and radius of gyration were used in Eq. (6.2.5.1a). It was observed that slenderness effects cannot be neglected; hence the column should be designed by considering the second-order effects.

The second step after slenderness is to investigate if the column should be analyzed as sway or non-sway. ACI CODE-440.11-22, Section 6.6.4.3 states that a column can be analyzed as part of a non-sway frame if: (a) column end moments due to second-order effects do not exceed 5% of the first-order end moments; and (b) the stability index

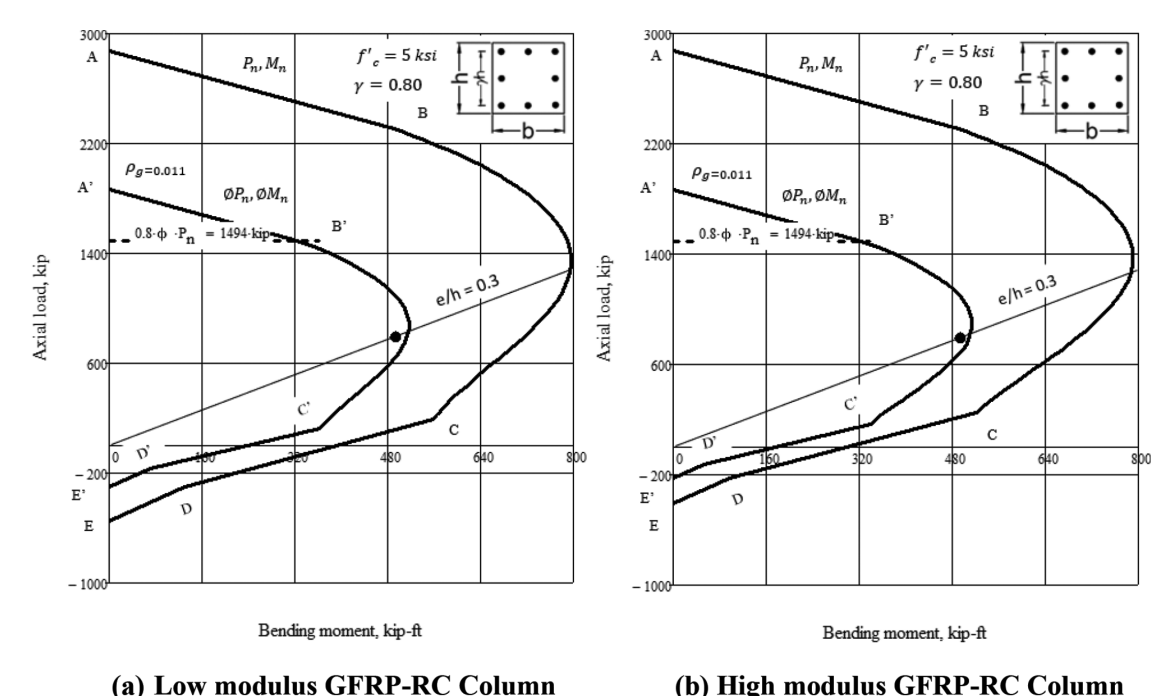


Fig. 3—Interaction diagram for GFRP-RC sway columns.

calculated as per 6.6.4.4.1 does not exceed 0.05. The sum of all factored column and wall gravity loads were considered as given in ACI 318-19 Design Handbook<sup>13</sup> equal to 25,700 kip (114,320 kN) and horizontal story shear equal to 775 kip (3450 kN). Because the first story of a building is often assumed hinged at  $0.67l_{u}$ , the following equation was used to calculate deflection at a distance l to the hinge

$$\delta_o = \frac{V_{us}l^3}{3\sum EI} \tag{13}$$

The deflection was found equal to 1.16 in. (29 mm), and the stability index (calculated as per Eq. (3)) was equal to 0.176, which is greater than 0.05; hence, the column was analyzed and designed as part of a sway frame. For a sway frame, the secondary moments at the end of the column due to differential movement of the ends of columns were calculated as per ACI CODE-440.11-22 Section 6.6.4.6.4 as given by Eq. (6a) and (6b) in this paper. The sway magnification factor was calculated as per Section 6.6.4.6.2, given as Eq. (7a) and (7b) in this paper. ACI CODE-440.11-22 allows three approaches for calculating moment magnifier, including: the Q method, the sum of P method, and secondorder elastic analysis. Because the example is based on hand calculations, the sum of P method was used to calculate sway magnification factor, as given by Eq. (7b). The critical buckling load can be calculated as per Section 6.6.4.4.2 in ACI CODE-440.11-22, given by Eq. (8) in this paper. The effective stiffness was calculated as per Section 6.6.4.4.4a, given by Eq. (9a), where factor  $B_{dns}$  was considered equal to zero for short-term lateral loads as allowed in ACI CODE-440.11-22, Section R6.6.4.6.2. The effective stiffness was calculated equal to  $36.8 \times 10^6$  kip-in.<sup>2</sup> ( $105.6 \times 10^9$  kN-mm<sup>2</sup>) and critical load equal to 1340 kip (5960 kN). The sway magnification factor calculated as per Eq. (7b) was equal

#### (b) High modulus GFRP-RC Column

to 2.5. The magnified moments calculated as per Section 6.6.4.6.1 were the lesser moment  $(M_1)$  equal to 368 kip-ft (500 kN-m) and the larger end moment ( $M_2$ ) equal to 493 kip-ft (670 kN-m).

ACI CODE-440.11-22, Section 10.6.1.1 states that area of longitudinal reinforcement shall be at least  $0.01A_g$ . Once the concrete cross-section dimensions and reinforcement amount are selected, the strength interaction diagram for that case is constructed by means of the spreadsheet specifically developed for GFRP-RC. The spreadsheet allows placing the reinforcement in the first  $(d_1)$  and last  $(d_n)$  layers as close to the outer column face as permitted by the Code. Bars could also be inserted along the two lateral sides of the cross section. The spreadsheet recomputes capacity resulting from changes in sectional strain to create a smooth plot of a nominal strength interaction diagram  $(P_n-M_n)$ . The values of nominal axial force and moment are multiplied by strength reduction factors, and limits on axial strength are applied to create the design strength interaction diagram ( $\phi P_n - \phi M_n$ ). As an example of the output of the spreadsheet, Fig. 3 shows the design interaction diagram developed for the 26 x 26 in. (660 x 660 mm) cross section of the sway column with reinforcement consisting of eight No. 9 (M29) bars for both lowand high-modulus GFRP. The horizontal dotted line in the interaction diagrams shows the limit on the nominal axial compressive strength to account for accidental eccentricities as per ACI CODE-440.11-22, Table 22.4.2.1 (that is, 0.8 for a column with ties).

The interaction diagram shown in Fig. 3 was constructed by locating critical points according to x (that is, the location of neutral axis) based on selected  $P_n$ - $M_n$  pairs. The two P-Mcurves show nominal strength (that is, points shown with plain letters A, B, C, D, and E) and design strength (that is, points shown with dashed letters A', B', C', D', and E'). Specifically, point A in Fig. 3 represents the maximum nominal

Table 5—Steel-RC and GFRP-RC sway column analysis and design

Column analysis					3		Column design						
Ultimate loads		Effective Moment magni- length factor fication factor		Steel-RC column			GFRP-RC column						
Applied load, kip	Moment, kip-ft	Steel	GFRP	Steel	GFRP	Magnified Size, Reinforcement moment, kip-ft in. area, in.2 (ratio, %)		Magnified moment, kip-ft	Size, in.	Reinforcement area, in. <sup>2</sup> (ratio, %)			
789	197	2.2	2.8	1.12	2.5	221	24 x 24	8 No. 8 (1.0)	493	26 x 26	8 No. 9 (1.1)		

Note: 1 kip = 4.44 kN; 1 kip-ft = 1.35 kN-m;  $1 \text{ in.}^2 = 645 \text{ mm}^2$ .

compressive force corresponding to zero eccentricity ( $M_n$  = 0 and  $x = + \frac{1}{4}$ ), which is the uppermost point in the interaction diagram. Point B' on the design domain limit represents the case of maximum compressive force usable in design. The two modes of failure (tension and compression-controlled modes) are separated by the "balanced failure" shown by point C', representing FRP rupture (note: the guaranteed strength of GFRP bars is replaced by  $0.01E_f$ , as specified in the Code) and concrete crushing simultaneously ( $x = x_b$ ). If the neutral axis shifts beyond  $x_b$ , the failure mode shifts from compression to tension. The lowermost point in the interaction diagram (E') corresponds to maximum tensile force ( $M_n$ = 0 and x = -Y), and maximum strain in the reinforcement. Any combination of ultimate axial load and moment (that is,  $P_u$ - $M_u$ , shown by a black dot) laying within the interaction curve represents safe (and outside, an unsafe) column

The GFRP-RC column subjected to same ultimate loads required larger cross section compared to steel-RC as the axial strength of GFRP reinforcement is not considered in resistance calculations and is replaced with equal area of concrete. Also, the higher magnification factor resulted in a very large, magnified moment, as given in Table 5, together with the limits on the maximum strength of GFRP bars, the GFRP-RC column required bigger cross-sectional dimensions than a steel-RC column. For example, a column designed with GFRP reinforcement failed with dimensions similar to that of the steel-RC (24 x 24 in. [610 x 610 mm]); therefore, the column size was increased to 26 x 26 in. (660 x 660 mm) to augment its load-carrying capacity to exceed the demand. The minimum reinforcement depends on the gross area of the cross section ( $A_{fmin} = 0.01A_g$ ); therefore, a GFRP-RC column required more reinforcement area than steel-RC. For example, a column designed with GFRP-RC required eight No. 9 (M29) bars, whereas that with steel-RC required eight No. 8 (M25) bars. The values of effective length factor, moment magnification factor, cross-sectional area, and longitudinal reinforcement for a column in sway frame are provided in Table 5, which includes values for steel-RC taken from ACI 318-19 Design Handbook.<sup>13</sup>

This study also investigated the effect of high-modulus ( $E_f$ = 8700 ksi [60,000 MPa]) GFRP reinforcement on column design. The compressive strength of GFRP reinforcement is not considered in resistance calculations when the GFRP is in compression (that is, the area of GFRP replaced with concrete); hence, the column dimensions remained same as with low-modulus GFRP bars (26 x 26 in. [660 x 660 mm]). Further, due to a limit on maximum GFRP tensile strain (that is, 0.01) by Code Section 10.3.2.1, only a slight increase in

the capacity (9%) for the column subjected to same demand (that is, as a low-modulus GFRP-RC column given in Table 5) was noticed. The column cross section, reinforcement details, and interaction diagrams developed for both low- and high-modulus GFRP-RC columns are shown in Fig. 3.

## Non-sway column using low- and high-modulus GFRP bars

The column example taken from the textbook by Wight and Macgregor<sup>15</sup> was redesigned with GFRP reinforcement, considering it as part of a non-sway frame as the stability index (Q = 0.04) and magnified moment were within the limits stated in Section 6.6.4.3 for a non-sway frame. The magnification factor calculated by analysis was 0.7; hence, a minimum magnification factor of 1.0 was used to calculate the magnified moment. The P-M diagram developed for non-sway columns showing the nominal and design capacity curves is shown in Fig. 4. The  $(P_n, M_n)$  curve shows the capacity before and  $(\Phi P_n, \Phi M_n)$  after the application of the strength reduction factors. The column failed with dimensions of the steel-RC section (14 x 14 in. [356 x 356 mm]) and reinforcement consisting of four No. 8 (M25) bars, as shown in Fig. 4(a), where the demand  $(P_u-M_u)$  shown by the black dot lies outside the design capacity curve. Therefore, the cross-section dimensions were increased to 18 x 18 in. (460 x 460 mm) and reinforcement consisting of four No. 9 (M29) bars to satisfy the demand. As shown in Fig. 4(b), the demand is within the design capacity curve, representing a safe column. It was observed that GFRP-RC columns require bigger cross sections and reinforcement areas than steel-RC. The effective length factor, moment magnification factor, cross-sectional dimensions, and required reinforcement are shown in Table 6.

Similar to the case of sway frames, an effort was made to investigate the impact of using high-modulus bars on non-sway column design. The high-modulus bars showed a 12% increase in the column capacity compared to low-modulus GFRP-RC column subjected to same demand (that is, the low-modulus GFRP-RC column given in Table 6). The column cross section, reinforcement details, and interaction diagrams developed for non-sway column are shown in Fig. 4.

#### PARAMETRIC STUDY

A parametric study was carried out by varying concrete compressive strength  $f_c$ , aspect ratio, and applied load eccentricity to evaluate implications on the design of GFRP-RC column cross sections. For comparison, steel-RC sections

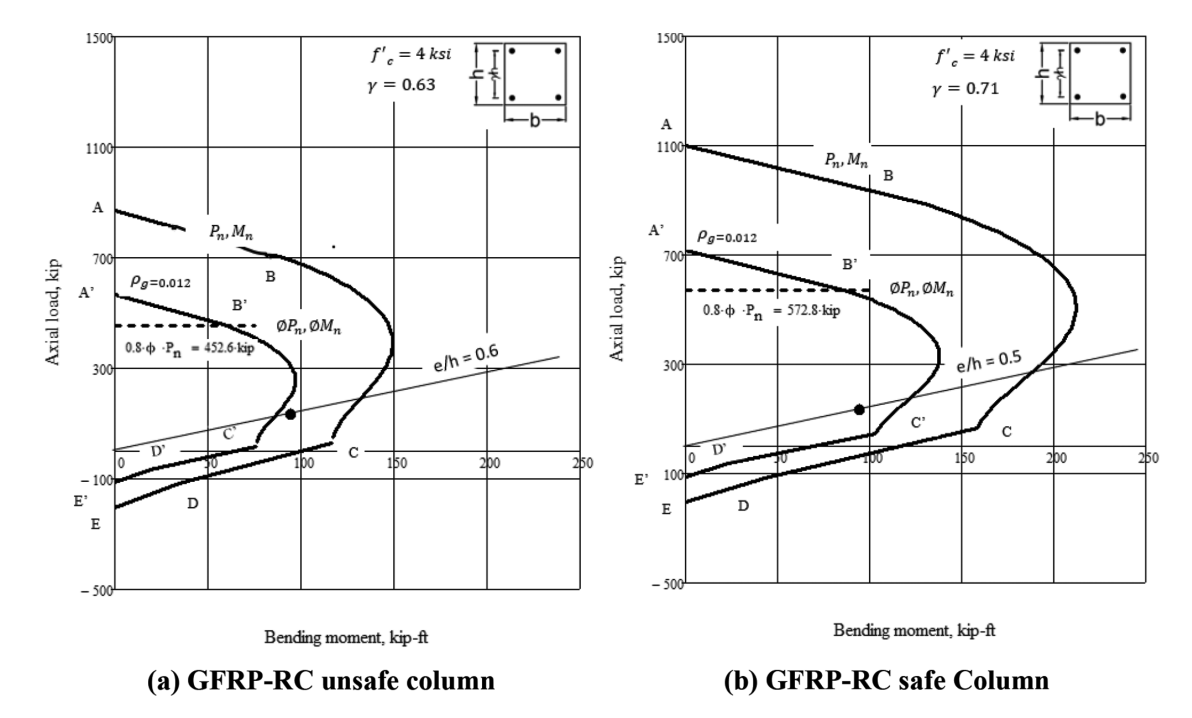


Fig. 4—Interaction diagram of GFRP-RC non-sway columns.

Table 6—Steel-RC and GFRP-RC non-sway column analysis and design

Column analysis					3	Column design						
			ective n factor			Steel-RC column			GFRP-RC column			
Applied load, kip	Moment, kip-ft	Steel	GFRP	Steel	GFRP	Magnified moment, kip-ft	Size, in.	Reinforcement area, in. <sup>2</sup> (ratio, %)	Magnified moment, kip-ft	Size, in.	Reinforcement area, in. <sup>2</sup> (ratio, %)	
134	94.4	0.77	0.80	0.53	0.7	94.4	14 x 14	4 No. 7 (1.2)	94.4	18 x 18	4 No. 9 (1.2)	

Note: 1 kip = 4.44 kN; 1 kip-ft = 1.35 kN-m;  $1 \text{ in.}^2 = 645 \text{ mm}^2$ .

were also designed by changing the parameters stated previously. The yielding strength of steel used was 60 ksi (414 MPa) and modulus of elasticity 29,000 ksi (200 GPa), whereas the GFRP reinforcement used was compliant with ASTM D7957 as referenced by ACI CODE-440.11-22. To compare results with steel-RC, both sections (steel-RC and GFRP-RC) were subjected to same demand (that is, no magnification factors were applied). Therefore, a cross section of 20 x 20 in. (508 x 508 mm) was used and varied as required. The reinforcement ratio was kept as close to minimum required 1% as possible throughout the parametric study.

#### Design with different $f_c$ values

Four different values of concrete strength ( $f_c' = 2500$ , 5000, 7500, and 10,000 psi [18, 35, 52, 70 MPa]) were used. The cross sections (steel-RC and GFRP-RC) were subjected to ultimate axial compressive load of 789 kip (3510 kN) and ultimate moment of 2367 kip-in. (267 kN-m) (no magnification factors applied). The reinforcement area was kept as close to 1% of gross concrete area as possible. As expected, RC cross-section dimensions significantly decreased with increasing concrete strength. For example, as shown in Table 7, at concrete strength of 5000 psi (3 MPa), the required GFRP cross section to satisfy the demand ( $P_u = 789$  kip [3510 kN] and  $M_u = 2367$  kip-in. [267 kN-m]) is

22 x 22 in. (560 x 560 mm), which decreased to 18 x 18 in. (460 x 460 mm) and 16 x 16 in. (406 x 406 mm) as concrete compressive strength increased to 7500 and 10,000 psi (52 and 70 MPa) respectively. Similarly, the required reinforcement decreased from six No. 9 (M29) bars at  $f_c' = 5000$  psi (35 MPa) to four No. 9 (M29) and four No. 8 (M25) at  $f_c' = 7500$  and 10,000 psi (52 and 70 MPa), respectively (note: reinforcement used at all three concrete strengths is  $1.2\%A_{\circ}$ ). It was further noticed that, at higher concrete strength, GFRP-RC sections performed similar to steel-RC. For example, as shown in Table 7, at  $f_c' = 5000 \text{ psi } (35 \text{ MPa})$ the required dimensions for GFRP-RC section are 22 x 22 in. (560 x 560 mm), whereas those for steel-RC are 20 x 20 in. (508 x 508 mm). However, when concrete strength increased to 7500 psi (52 MPa) and above, the required dimensions for both RC sections are the same.

In contrast, when concrete strength was decreased to 2500 psi (18 MPa), the required cross sections significantly increased to satisfy the demand. Similar effects were observed in the case of steel-RC; however, unlike steel-RC, GFRP-RC dimensions and reinforcement area increased more rapidly. For example, the steel-RC section satisfied the demand with cross-sectional dimensions equal to 26 x 26 in. (660 x 660 mm) with eight No. 9 (M29) bars ( $\rho$  = 0.011 $A_g$ ), whereas GFRP-RC required 28 x 28 in. (710 x 710 mm) with eight No. 9 (M29) bars ( $\rho$  = 0.01 $A_g$ ). It has

Table 7—Cross sections at different  $f_{c'}$  values

Demand				Steel-RC			GFRP-RC			
Applied load, kip	Ultimate moment, kip-in.	Eccentricity, in.	Concrete strength, psi	h/6	Size, in.	Reinforcement area, in. <sup>2</sup> (ratio, %)	h/6	Size, in.	Reinforcement area, in. <sup>2</sup> (ratio, %)	
			$f_c' = 2500$	4.3	26 x 26	8 No. 9 (1.1)	4.6	28 x 28	8 No. 9 (1.0)	
700	2267	2.0	$f_c' = 5000$	3.3	20 x 20	4 No. 9 (1.0)	3.6	22 x 22	6 No. 9 (1.2)	
789	2367	3.0	$f_c' = 7500$	3.0	18 x 18	4 No. 9 (1.2)	3.0	18 x 18	4 No. 9 (1.2)	
			$f_c' = 10,000$	2.7	16 x 16	4 No. 8 (1.2)	2.7	16 x 16	4 No. 8 (1.2)	

Note: 1 kip = 4.44 kN; 1 kip-in. = 113 kN-mm; 1 in. = 25.4 mm; 1 in.  $^2$  = 645 mm<sup>2</sup>.

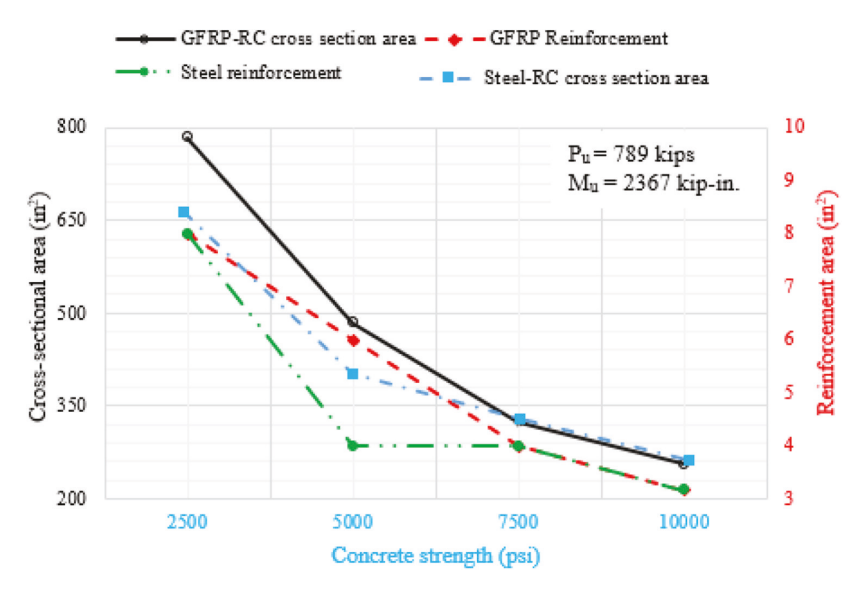


Fig. 5—Cross sections at different f<sub>c</sub>' values.

been noted that higher concrete strengths have profound effects on cross-sectional dimensions and reinforcement area of GFRP-RC. The effect of changing concrete strength on cross-sectional dimensions and reinforcement area can be visualized in Table 7 and Fig. 5.

Also, it is worth noting here that kern distance significantly decreases with increasing concrete strength. For example, for GFRP-RC, at  $f_c' = 5000$  psi (35 MPa), the applied axial load acts at e = 3.0 in. (76 mm), which is within kern distance (h/6 = 3.6 in. [92 mm]), implying that the axial load does not cause tension in the section. However, at a concrete strength of 7500 psi (52 MPa), the kern distance significantly decreased and ultimately, the eccentricity falls outside the kern (e = 3.0 in. [76 mm] and h/6= 2.7 in. [69 mm]) when  $f_c' = 10,000$  psi (70 MPa). Therefore, as observed by calculations, higher concrete strength help decreasing cross-sectional dimensions and axial load causes tension in the section. Subsequently, GFRP-RC cross sections take advantage of tensile properties of GFRP reinforcement and require dimensions similar to steel-RC. For example, as shown in Table 7, at  $f_c' = 7500$  and 10,000 (52) and 70 MPa), GFRP-RC required cross-sectional areas of 18 x 18 in. (460 x 460 mm) and 16 x 16 in. (406 x 406 mm) and reinforcement of four No. 9 (M29) and four No. 8 (M25) bars, respectively—the same as steel-RC.

#### Design with different cross-section aspect ratio

The cross-section aspect ratio was changed from 1.0 to 1.5 and 2.0. The ultimate axial load and moment were kept same for both RC cross sections (steel-RC and GFRP-RC) with no magnification factors applied ( $P_u = 789 \text{ kip } [3510 \text{ kN}], M_u = 2367 \text{ kip-in.} [267 \text{ kN-m}]$ ). The reinforcement ratio was kept as close to 1% of the gross concrete area as possible and concrete strength was 5000 psi (35 MPa).

As expected, when changing the cross-section aspect ratio from 1.0 to 1.5 and 2.0, the required dimensions for both RC sections decreased. For example, as shown in Table 8, the GFRP-RC cross-sectional area decreased to 17 x 26 in. (432 x 660 mm) from 22 x 22 in. (560 x 560 mm) and steel-RC to 16 x 24 in. (406 x 610 mm) from 20 x 20 in. (508 x 508 mm) when changing aspect ratio from 1.0 to 1.5. It further decreased to 14 x 28 in. (356 x 710 mm) and 13 x 26 in. (330 x 660 mm) for GFRP-RC and steel-RC, respectively, when increasing the aspect ratio to 2.0. It can be observed in Table 8 that the required dimensions and reinforcement area for GFRP-RC are larger than steel-RC for the three aspect ratios investigated. It should be noted that, in all three cross sections the axial load is applied at e = 3.0 in. (76 mm), which falls within the kern distance (h/6). This implies that the applied load does not cause tension in the cross section. The effect of changing the aspect ratio may be more prominent for GFRP-RC cross sections subjected to highly eccentric loads (that is, eccentricity exceeding kern distance h/6). Therefore, an attempt was made to investigate the cross

Table 8—Cross sections at different aspect ratios

Demand				Steel-RC				GFRP-RC			
Applied load, kip	Ultimate moment, kip-in.	Eccentricity, in.	Aspect ratio	h/6	Size, in.	Reinforcement area, in.² (ratio, %)	h/6	Size, in.	Reinforcement area, in. <sup>2</sup> (ratio, %)		
		1.0	3.3	20 x 20	4 No. 9 (1.0)	3.7	22 x 22	6 No. 9 (1.2)			
789	2367	3.0	1.5	4.0	16 x 24	4 No. 9 (1.0)	4.3	17 x 26	6 No. 8 (1.0)		
			2.0	4.3	13 x 26	4 No. 9 (1.1)	4.6	14 x 28	4 No. 9 (1.0)		
			1.0	3.0	18 x 18	4 No. 9 (1.2)	3.0	20 x 20	4 No. 9 (1.0)		
395	2367	6.0	1.5	3.7	14 x 22	4 No. 8 (1.0)	3.7	14 x 22	4 No. 8 (1.0)		
			2.0	4.0	12 x 24	4 No. 8 (1.0)	4.0	12 x 24	4 No. 8 (1.0)		

Note: 1 kip = 4.44 kN; 1 kip-in. = 113 kN-mm; 1 in. = 25.4 mm;  $1 \text{ in.}^2 = 645 \text{ mm}^2$ .

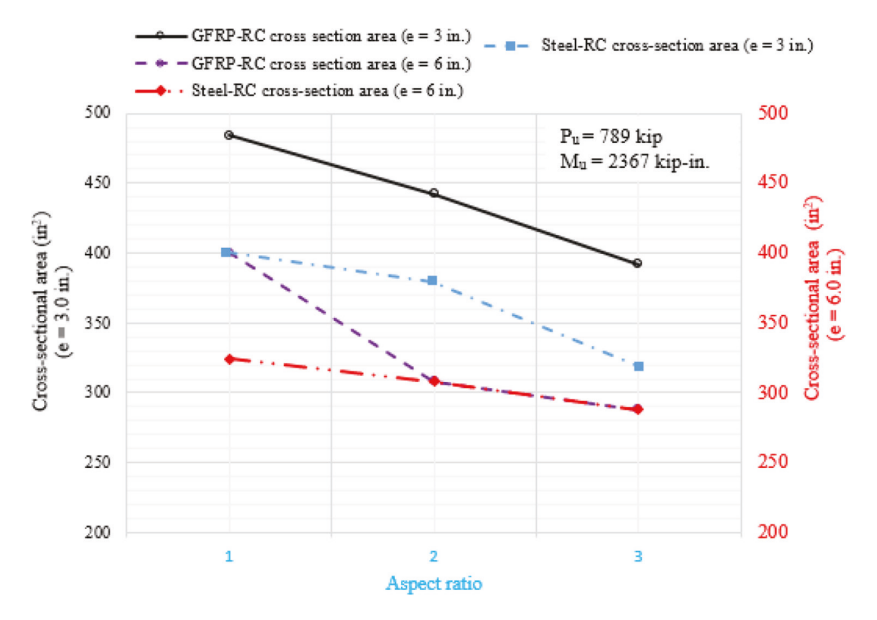


Fig. 6—Cross sections at different aspect ratios.

sections by increasing the eccentricity to 6.0 in. (152 mm). The axial load was decreased to half (395 kip [1760 kN]) while moment was kept the same (2367 kip-in. [267 kip-ft]). For the GFRP-RC, it was observed that at an aspect ratio of 1.0, the required dimensions decreased to satisfy the demand (20 x 20 in. [508 x 508 mm] from 22 x 22 in. [560 x 560 mm]), as the axial load decreased to half of original load). It was further observed that for GFRP-RC the required dimensions and reinforcement area significantly decreased with increasing aspect ratio and were similar to steel-RC at aspect ratios equal to 1.5 and 2.0. For example, as shown in Table 8, at aspect ratios of 1.5 and 2.0, the required dimensions for GFRP-RC are 14 x 22 in. (356 x 560 mm) and 12 x 24 in. (305 x 610 mm), which are 23% and 28% less from a cross section with an aspect ratio of 1.0 (that is, 20 x 20 in. [508 x 508 mm]) and are the same as steel-RC at same aspect ratios. For all three aspect ratios, the eccentricity is outside the kern distance (h/6), implying that there is tension in the cross sections. Figure 6 shows the trend of changing the cross-sectional area when increasing the aspect ratio at eccentricities of 3.0 and 6.0 in. (76 and 152 mm).

#### Design with different load eccentricities

The analysis was carried out with the intent of changing eccentricities by altering the values of axial load

while keeping the moment constant ( $M_u = 2367$  kip-in. [267 kN-m]), with no magnification factors applied, to evaluate the effect on cross-sectional dimensions and reinforcement area. The eccentricities were gradually enhanced at increments of 0.5 in. (13 mm), except for the points inside (0.1h), exactly on (h/6), and outside (0.2h) the kern (note: the kern distances are based on GFRP-RC cross-section dimensions). For square cross sections, the eccentricity values used in the calculations are 1.0., 1.5, 2.0, 2.4, 2.5, 3.0, 3.6, and 4.0. The reinforcement ratio was kept as close to a minimum 1% of the gross concrete area as possible and the concrete strength used was 5000 psi (35 MPa). To compare the efficacy of GFRP-RC, steel-RC cross sections were also designed by changing the same parameters as stated previously. It should be noted that both RC sections were subjected to same demand (that is, no magnification factors were applied).

The cross-section design started with minimum cross-sectional area sufficient to satisfy the demand at e = 1.0 in. (25.4 mm), as shown in Table 9. It can be observed in Table 9 that when axial loads are high, the required cross-sectional dimensions for GFRP-RC increase more rapidly compared to steel-RC. For example, at an eccentricity value equal to 1.0 in. (25.4 mm) ( $P_u = 2367 \text{ kip } [10,530 \text{ kN}]$ ), the required dimensions for GFRP-RC are 34 x 34 in. (860 x 860 mm),

Table 9—Cross sections with different eccentricities at constant moment

			Steel-RC		GFRP-RC				
Eccentricity, in.	Ultimate load, kip	e/h	Cross-section area, in.	Reinforcement area, in. <sup>2</sup> (ratio, %)	e/h	Cross-section area, in.	Reinforcement area, in. <sup>2</sup> (ratio, %)		
1.0	2367	0.03	32 x 32	12 No. 9 (1.1)	0.03	34 x 34	12 No. 9(1.0)		
1.5	1578	0.05	26 x 26	8 No. 9 (1.1)	0.05	28 x 28	8 No. 9(1.0)		
2.0	1184	0.09			0.08	24 x 24	(N 0(10)		
2.4 (0.1 <i>h</i> )	1075	0.10	22 x 22	6 No. 9 (1.2)	0.10	24 X 24	6 No. 9(1.0)		
2.5	947	0.11			0.11	22 x 22	(N- 0(12)		
3.0	789	0.15			0.13	22 X 22	6 No. 9(1.2)		
3.6 (h/6)	710	0.18	20 x 20	4 No. 9 (1.0)	0.18	20 20	4 N - 0(1 0)		
4.0 (0.2 <i>h</i> )	592	0.2			0.2	20 x 20	4 No. 9(1.0)		

Note: 1 in. = 25.4 mm; 1 kip = 4.44 kN; 1 in.<sup>2</sup> = 645 mm<sup>2</sup>.

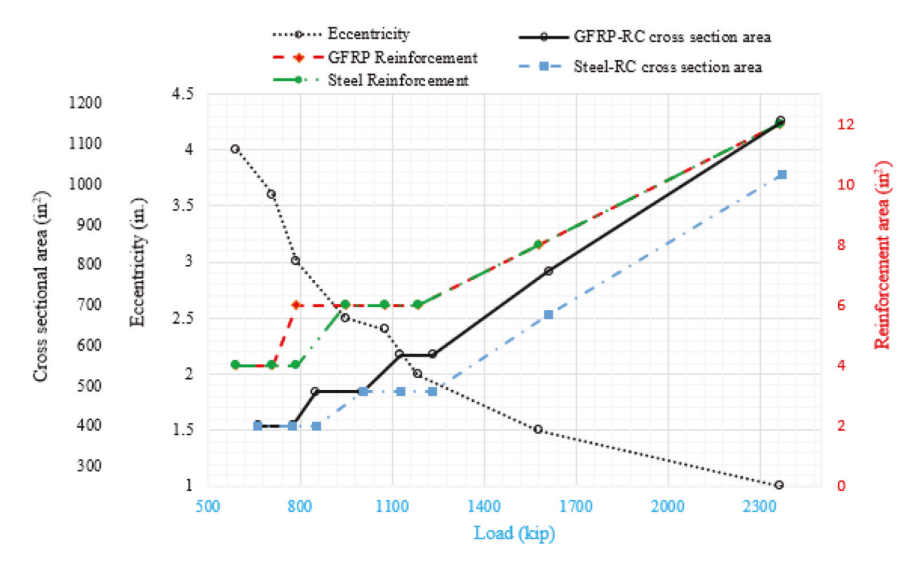


Fig. 7—Cross sections with different eccentricities at constant moment.

and those for steel-RC are 32 x 32 in. (812 x 812 mm). However, when the eccentricity value increases to 4.0 in. (100 mm), the required dimensions for two RC sections are the same. Similarly, the required reinforcement area also decreases and is the same for GFRP-RC and steel-RC (four No. 9 [M29] bars). Despite stricter design limits compared to steel-RC, the GFRP was found effective to resist loads with high eccentricities, especially for values exceeding the kern distance (h/6). For example, in Table 9, at eccentricity e = 4.0 in. (100 mm), the axial load acts outside the kern distance (h/6 = 3.6), causing tension in the cross section and requires that cross-section dimensions for two RC sections are same. The required reinforcement and cross-sectional area with changing eccentricity values can be seen in Table 9 and increase in reinforcement requirements and crosssectional area with increasing eccentricities are visualized in Fig. 7.

# COLUMN PROVISIONS FOR SHEAR IN CODE-440.11-22

ACI CODE-440.11-22 Section 10.5.3.1 references Section 22.5 for the calculation of nominal shear strength of column, which can be calculated as given in Section 22.5.1.1

$$V_n = V_c + V_f \tag{14}$$

where  $V_n$  is nominal shear strength;  $V_c$  is nominal shear strength provided by the concrete; and  $V_f$  is nominal shear strength provided by GFRP shear reinforcement.

The shear strength provided by concrete is calculated as the greater of two expressions, given by Code Sections 22.5.5.1a and 22.5.5.1b as follows

$$V_c = 5\lambda k_{cr} \sqrt{f_c}' bd$$
 (US units)  
 $V_c = 0.42\lambda k_{cr} \sqrt{f_c}' bd$  (SI units) (15a)

$$V_c = 0.8\lambda \sqrt{f_c}'bd$$
 (US units)  
 $V_c = 0.066\lambda \sqrt{f_c}'bd$  (SI units) (15b)

where  $k_{cr}$  is ratio of the depth of elastic cracked section neutral

axis to the effective depth given by the Code Commentary Section R22.5.5.1, shown as follows

$$k_{cr,rect} = \sqrt{2 \rho_f n_f + (\rho_f n_f)^2} - \rho_f n_f$$

where  $\rho_f = (A/bd)$  is the reinforcement ratio;  $A_f$  is the area of GFRP reinforcement;  $n_f = (E/E_c)$  is the modular ratio; and  $E_c$  is the concrete elastic modulus calculated as given by Code Section 19.2.2.1

$$E_c = 57,000\sqrt{f_c} \quad \text{(US units)}$$

$$E_c = 4700\sqrt{f_c} \quad \text{(SI units)}$$
(17)

and  $\lambda = \sqrt{2/(1 + [d/10])} (\sqrt{2/(1 + 0.004d)})$  is the size effect factor as given in ACI CODE-440.11-22, Section 22.5.5.1.3.

The size effect factor was considered for these examples because h exceeded 10 in. (254 mm).

The shear strength provided by the GFRP reinforcement is as given in Code Section 22.5.8.5.3

$$V_f = A_{fi} f_{fi}(d/s) \tag{18}$$

where  $A_{fv}$  is the area of shear reinforcement as given in Code Commentary Eq. (R22.5.8.5)

$$\frac{A_{fv}}{S} = \frac{V_u - \Phi V_c}{\Phi f_f d} \tag{19}$$

and  $f_{ft}$  is the permissible stress in the GFRP shear reinforcement. The design tensile strength of GFRP transverse reinforcement is controlled by the strength of the bent portion of the bar and by a strain limit of 0.005, as given by Code Section 20.2.2.6

$$f_{ft} \le (f_{fb}, 0.005E_f)$$
 (20)

where  $f_{fb}$  is the guaranteed ultimate tensile strength of the bent portion of the bar. Its minimum value be taken as specified in ASTM D7957; and s is center-to-center spacing of transverse reinforcement.

Maximum spacing  $s_{max}$  between legs of shear reinforcement is calculated as the least of maximum spacing limitations given by Code in 10.6.2.2 and its Commentary in R22.5.8.5

$$s_{max} = \frac{A_{fv} \Phi f_{ft} d}{V_u - \Phi V_c} \tag{21}$$

$$s_{max} = \frac{A_{fi}f_{fi}}{0.75\sqrt{f_c}b} \quad \text{(US units)}$$

$$s_{max} = \frac{A_{fi}f_{fi}}{0.062\sqrt{f_c}b} \quad \text{(SI units)}$$

$$s_{max} = \frac{A_{fi}f_{fi}}{50b} \quad \text{(US units)}$$

$$s_{max} = \frac{A_{fi}f_{fi}}{0.35b} \quad \text{(SI units)}$$
(22b)

The maximum tie spacing requirement is also provided in the Code Section 22.7.2.1. The maximum tie spacing shall not exceed  $12d_b$  of longitudinal bar,  $24d_b$  of tie bar, h, or b.

#### **EXAMPLE OF SHEAR DESIGN AND DISCUSSION**

The sway GFRP-RC column was designed for gravity load and magnified moment ( $P_u = 789 \text{ kip } [3510 \text{ kN}], M_u =$ 493 kip-ft [670 kN-m]) that required a cross-sectional area equal to 26 x 26 in. (660 x 660 mm). This section discusses the shear design of the aforementioned cross section subjected shear force  $(V_{\mu})$  of magnitude 22 kip (98 kN), as given in Table 4. The shear strength provided by the concrete cross section ( $\Phi V_c$ ) was calculated with Eq. (22.5.5.1a) and (22.5.5.1b), as given in column provisions for shear. The GFRP bars used as transverse reinforcement were compliant with ASTM D7957, 12 which states that the guaranteed ultimate tensile force of the bent portion of a bar shall be greater than or equal to 60% of the values of guaranteed ultimate tensile force provided in ASTM D7957, Table 3.12 Also, for transverse reinforcement, No. 4 (M13) bars were used, having a minimum inside diameter of the bend equal to 3 in. (76 mm) as given in ASTM D7957, Table 4.12

It was observed from the calculations that shear strength provided by the concrete cross section alone is not sufficient to resist the shear force. Hence the shear capacity must increase by means of shear reinforcement to satisfy the shear demand. It should be noted that limits on the shear strength provided by concrete resulted in lower  $V_c$  together with a 40% reduction in the strength at the bend of GFRP transverse reinforcement 12 significantly affect shear design. The limits on the maximum strength of GFRP transverse reinforcement given by Code Section 20.2.2.6 only allowed the maximum design tensile strength of reinforcement equal to 32.5 ksi (224 MPa), which is 70% less than actual strength value of No. 4 (M13) bars.

In this column example, to augment the shear strength of the cross section, No. 4 (M13) bars were used at 9 in. (228 mm) center-to-center. Whereas the same column when designed with steel-RC only required minimum shear reinforcement (that is, No. 4 [M29] at 16 in. [406 mm] center-to-center) to hold the longitudinal reinforcement, as the shear strength provided by the concrete cross section for steel-RC (24 x 24 in. [610 x 610 mm]) was sufficient to satisfy the shear demand.

The Code Sections 25.7.2.3a, 25.7.2.3b, and 25.7.2.3c require that lateral support from ties be provided for bars at every corner, and to bars with greater than 6 in. (152 mm) clear on each side. Therefore, in this column example, two C-shaped tie bars forming a diamond shape for middle longitudinal bars, in addition to two overlapping C-shaped tie bars for corner longitudinal reinforcement, were used, as shown in Fig. 8. The tie size, its dimensions, and their distribution along column height are schematically shown in Fig. 8 for a sway column.

The non-sway GFRP-RC column was subjected to an axial compressive load of 134 kip (596 kN), magnified moment of 94.4 kip-ft (128 kN-m), and no shear force value is specified in reference source. To resist the gravity load and applied moment, the column required a cross-sectional area equal to 18 x 18 in. (460 x 460 mm) and four No. 9 (M29) longitudinal bars. Though no shear force is given in the column example, minimum reinforcement was still used to hold the longitudinal bars in position and avoid buckling.

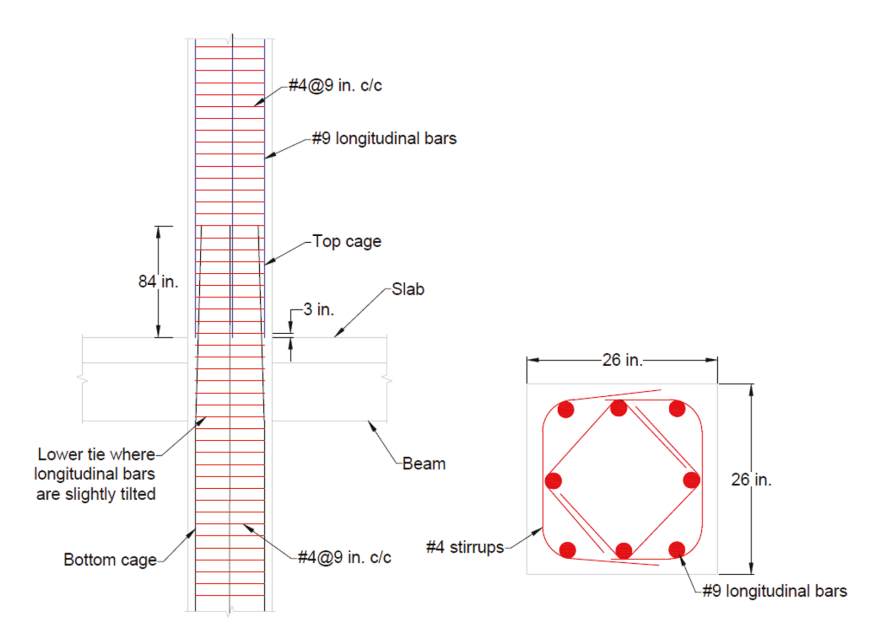


Fig. 8—Schematic of reinforcement details in sway GFRP-RC column.

The transverse reinforcement was used at maximum specified spacings as given in Code Sections 10.6.2.2 and 25.7.2.1 and Code Commentary Section R22.5.8.5.

In this column, for transverse reinforcement, No. 4 (M13) bars having an inside bend diameter equal to 3 in. (76 mm) as stated in ASTM D7957,  $^{12}$  Table 4 was used. As mentioned in previous sections, the maximum spacing of ties cannot exceed  $12d_b$ , 24 diameter of tie bar, and the smallest dimensions of the member. Therefore, with the given cross-section dimensions and longitudinal reinforcement information in this column example, No. 4 (M13) ties were used at 12 in. (300 mm) center-to-center.

#### COLUMN PROVISIONS FOR DETAILING IN CODE-440.11-22

Code Section 25.4.1.1 requires that tension or compression reinforcement at each section of a member shall be developed on each side of that section by embedment length, hook, mechanical device, or a combination thereof. Development length  $l_d$  for bars in tension shall be greater of the values calculated by Code Sections 25.4.2.1(a), 25.4.2.1(b), and 25.4.2.1(c)

$$l_d = \frac{d_b \left(\frac{f_{fr}}{\sqrt{f_c}} - 340\right)}{13.6 + \frac{c_b}{d_b}} \omega \qquad \text{(US units)}$$

$$l_d = \frac{d_b \left(\frac{f_{fr}}{0.083\sqrt{f_c}} - 340\right)}{13.6 + \frac{c_b}{d_b}} \omega \qquad \text{(SI units)}$$

in which  $c_b/d_b$  shall not be taken greater than 3.5, and where  $c_b$  is the lesser of: (a) the distance from center of a bar to nearest concrete surface, and (b) one-half the center-center spacing of bars being developed;  $d_b$  is the nominal bar

diameter;  $f_{fr}$  is the GFRP tensile stress required to develop the full nominal section capacity;  $\omega$  is the bar location modification factor, taken equal to 1.5, if more than 12 in. (300 mm) of fresh concrete is placed below the reinforcement being developed and 1.0 for all other cases.

$$20d_{b}$$
 (23b)

The lap splice lengths in columns shall be calculated in accordance with 10.7.5 and 25.5. Code Section 10.7.5.2 states that in a column subjected to moment and axial force, tensile stresses may occur on one face of the column for moderate or large eccentricities. If such stresses occur, Code Section 10.7.5.2.2 requires tension splices to be used, which can be classified as Class A or Class B lap splices and calculated in accordance with Code Section 25.5.2.1, as given in Table 10.

Code Section 10.7.5.2.1 states that if the bar is compressive due to factored loads, compression lap splices shall be permitted. Given no experimental data on development length for GFRP bars in compression ( $l_{dc}$ ), Code Section 25.4.9.1 states that the development length in compression shall be conservatively taken the same as that for tension as in Code Section 25.4.2.1.

The minimum overlap of tie bar ends shall be greater of  $20d_b$  or 6 in. (152 mm), as in 25.7.2.3.1.

Code Section 10.7.6.2 states that the bottom tie shall be located not more than one-half the tie spacing above the top of footing or slab; similarly, the top tie shall be located not more than one-half the tie spacing below the lowest horizontal reinforcement in the slab, drop panel, or shear cap. If beams frame into all sides of column, the top tie shall be located not more than 3 in. (76 mm) below the lowest horizontal reinforcement in the shallowest beam.

Table 10—Lap splice length of GFRP bars in tension (ACI CODE-440.11-22, Section 25.5.2.1)

$A_{f,provided}/A_{f,required}^*$ over length of splice	Maximum percent of $A_f$ spliced within required lap length	Splice type		$l_{st}$
>2.0	50	Class A	Greater of:	$1.0l_d$ , $20d_b$ , and 12 in.
≥2.0	100	Class B	Cuantam of	1.27. 20.4. and 12 in
<2.0	All classes	Class B	Greater of:	$1.3l_d$ , $20d_b$ , and 12 in.

<sup>\*</sup>Ratio of area of reinforcement provided to area of reinforcement required by analysis at splice location.

Note: 1 in. = 25.4 mm.

### DETAILING OF REINFORCEMENT FOR COLUMN EXAMPLES

The Code permits the use of the same equation for development lengths of GFRP bars in compression and tension (Eq. (25.4.2)). Therefore, the development length equation for GFRP bars was conservatively adopted as given in Code Section 25.4.2. Also, there is more than 12 in. (300 mm) of fresh concrete to be placed below the longitudinal bar being developed in a sway column; hence, the bar location modification factor ( $\omega = 1.5$ ) was also used. The Code specifies a maximum limit for the term  $c_b/d_b$  as 3.5, which in this column resulted as 1.83, well below the permitted limit. The development length was calculated using three equations mentioned in Code Section 25.4.2 and Eq. (25.4.2.1(a)) governed, which resulted in 64 in. (1625 mm).

The tensile bar stress at a point reaches its maximum value (limited by maximum strain 0.01), which is greater than  $0.5f_{fii}$ ; also, the ratio of area of reinforcement provided to the area of reinforcement required in this example is less than 2.0 (that is, 1.18); therefore, Class B lap splices were used. The splice length was calculated as given in Code Section 25.5.2.1 (that is, the greater of  $1.3l_d$ ,  $20d_b$ , and 12 in. [300 mm]), which resulted 84 in. (3134 mm).

The lap splice calculated for the steel-RC column was 33 in. (840 mm), which shows that GFRP-RC columns require very large splice lengths (2.5 times greater than steel-RC). Unlike steel, GFRP bars cannot be bent on site and together with more GFRP reinforcement required, they increase the complexity in cage preparation. It is the sole responsibility of the contractor to splice column reinforcement cages. As shown in Fig. 7, the bottom cage bars are shown slightly tilted just after the start of the beam to differentiate from top bars.

Code Section 10.7.6.2 explains the distribution of ties in a beam-column joint. It states that the bottom tie shall be located not more than one-half the tie spacing above the top of footing or slab; similarly, the top tie shall be located not more than one-half the tie spacing below the lowest horizontal reinforcement in the slab, drop panel, or shear cap. In this example, the first tie was placed at 3 in. (76 mm) from the floor top, followed by others at the required spacing. Two pieces of C-shaped stirrups with minimum overlap as the greater of  $20d_b$  and 6 in. (152 mm) were used as per Code Section 25.7.2.3.1. In current column design, No. 4 (M13) bars are used; hence, an overlap of 10 in. (254 mm) is provided.

The development length for non-sway GFRP-RC column (18 x 18 in. [460 x 460 mm]) was calculated using Code-specified Eq. 25.4.2.1(a), 25.4.2.1(b), and 25.4.2.1(c).

The development length equation for GFRP bars in tension (Eq. (25.4.2a)) was conservatively adopted for this case as well. Also, the bar location modification factor ( $\omega = 1.5$ ) was used to calculate the development length. The term  $c_b/d_b$  in this column resulted in 1.83, which is well below the permissible limit of 3.5. The development length calculated for non-sway column as per Code Section 25.4.2 resulted in 75 in. (1900 mm). Because the tensile bar stress reaches its full capacity at a point (limited by maximum strain 0.01) which is greater than  $0.5f_{fit}$ , and the ratio of area of reinforcement provided to area of reinforcement required is less than 2.0, therefore, Class B lap splices were selected. The splice length was calculated as given in Code Section 25.5.2.1, which resulted a value equal to 98 in. (2490 mm).

Code Section 10.7.6.2 explains the distribution of ties in a beam-column joint. The first tie was conservatively placed at 3 in. (76 mm), as required by Code Section 10.7.6.2, followed by the required spacing. C-shaped ties were used in the non-sway column, with an overlap as stated in Code Section 25.7.2.3.1, which resulted in 10 in. (254 mm) when using No. 4 (M13) ties.

#### CONCLUSIONS AND RECOMMENDATIONS

In this study, a sway column example originally designed with steel reinforcement was taken from the ACI Design Handbook,<sup>13</sup> a companion to ACI 318-19,<sup>14</sup> and a non-sway column example from the textbook by Wight and Macgregor.<sup>15</sup> These two columns were redesigned with glass fiber-reinforced polymer (GFRP) reinforcement to show the implications of ACI CODE-440.11-22<sup>11</sup> with both low- ( $E_f$ = 6500 ksi [44,815 MPa]) and high-modulus ( $E_f$  = 8700 ksi [60,000 MPa]) GFRP bars. A limited parametric study was carried out to evaluate the effects of changing values of  $f_c$ ', cross-section aspect ratio, and eccentricity. Based on the outcomes of this study, the following conclusions were drawn:

- The stiffness values for GFRP reinforcement result in higher moment magnification factors for GFRP-reinforced concrete (RC) compared to steel-RC columns.
- The advantage of high modulus/strength of new-generation GFRP bars can be beneficial to resist conditions of large eccentricities. However, due to limits on maximum tensile strain (0.01 in./in. [0.01 mm/mm]) to control column curvature, these benefits are not fully used.
- The compressive strength and stiffness of GFRP reinforcement is replaced with an equal area of concrete; hence, bigger cross sections are typically required for GFRP-RC columns when compared to steel-RC.

- Minimum reinforcement depends on the concrete gross area; hence, because of larger cross-section dimensions, GFRP-RC will require more reinforcement than steel-RC
- It is obvious that increasing concrete strength helps decrease dimensions of RC sections. However, the concrete strength has an additional effect on the performance GFRP-RC cross sections. For the case considered and at concrete strength of 7500 psi (52 MPa) and above, the required dimensions for steel-RC and GFRP-RC were the same, as opposite at lower concrete strengths.
- As expected, the rectangular sections performed better than square sections, and in most cases, GFRP-RC and steel-RC required the same cross sections when axial load acted outside the kern (that is, large eccentricities).
- The current development length equation in the Code result in very large values compared to steel-RC because there is no distinction in the requirements for compression and tension splices. Research should be undertaken to reassess provision parameters by incorporating improvements in material properties.
- It is observed that replacing the contribution of GFRP reinforcement in compression with an equal area of concrete significantly affected the design. With the recent advancements in material properties and manufacturing techniques, there is need to re-investigate the contribution of GFRP bars in the axial compressive capacity of GFRP-RC columns using high-modulus GFRP reinforcement.

#### **AUTHOR BIOS**

Zahid Hussain is a PhD Student in Civil and Architectural Engineering Department at the University of Miami, Coral Gables, FL. He is a member of ACI Committee 440, Fiber Reinforced Polymer Reinforcement. His research interests include sustainable materials, computational methods, design, and behavior of fiber-reinforced polymer (FRP)-reinforced structures.

Antonio Nanni, FACI, is an Inaugural Senior Scholar, Professor, and Chair of the Department of Civil and Architectural Engineering at the University of Miami. He is a member of ACI Committees 440, Fiber Reinforced Polymer Reinforcement, and 549, Thin Reinforced Cementitious Products and Ferrocement.

#### **ACKNOWLEDGMENTS**

The authors would like to thank the National Science Foundation, Grant No. 1916342, and the Higher Education Commission of Pakistan for their financial support of the lead author.

#### **REFERENCES**

- 1. ACI Committee 440, "Guide for the Design and Construction of Structural Concrete Reinforced with Fiber-Reinforced Polymer (FRP) Bars (ACI 440.1R-15)," American Concrete Institute, Farmington Hills, MI, 88 pp.
- 2. Zhang, P.; Lv, X.; Zhang, H.; Liu, Y.; Chen, B.; Gao, D.; and Shaikh, S. A., "Experimental Investigations of GFRP Reinforced Columns with Composite Spiral Stirrups under Concentric Compression," *Journal of Building Engineering*, V. 46, No. 4, 2022, pp. 1-21. doi: 10.1016/j. jobe.2021.103768
- 3. Hasan, H. A.; Sheikh, M. N.; and Hadi, M. N. S., "Performance Evaluation of High Strength Concrete and Steel Fiber High Strength Concrete Columns Reinforced with GFRP Bars and Helices," *Construction and Building Materials*, V. 134, No. 2, 2017, pp. 297-310. doi: 10.1016/j. conbuildmat.2016.12.124
- 4. De Luca, A.; Matta, F.; and Nanni, A., "Behavior of Full Scale GFRP Reinforced Concrete Columns under Axial Load," *ACI Structural Journal*, V. 107, No. 2, Mar.-Apr. 2010, pp. 589-596.
- 5. De Luca, A.; Matta, F.; and Nanni, A., "Structural Response of Full Scale Reinforced Concrete Columns with Internal FRP Reinforcement under Compressive Load," 9th International Symposium on Fiber Reinforced Polymer Reinforcement for Concrete Structures, D. Oehlers, M. Griffith, and R. Seracino, eds., Sydney, Australia, July 13-15, 2010.
- 6. Jawaheri Zadeh, H., and Nanni, A., "Flexural Stiffness and Second Order Effects in FRP-RC Frames," *ACI Structural Journal*, V. 114, No. 2, Mar. 2017, pp. 533-544.
- 7. Bischoff, P. H., "Member Stiffness for Frame Analysis for GFRP Reinforced Concrete Structures," *IABSE Symposium—Engineering the Future*, Sept. 21-23, 2017.
- 8. Hadhood, A.; Mohamed, H. M.; Benmokrane, B.; Nanni, A.; and Shield, C. K., "Assessment of Design Guidelines of Concrete Columns Reinforced with Glass Fiber-Reinforced Polymer Bars," *ACI Structural Journal*, V. 116, No. 4, July 2019, pp. 193-207. doi: 10.14359/51715663
- 9. Guérin, M.; Mohamed, H. M.; Benmokrane, B.; Shield, C. K.; and Nanni, A., "Effect of Glass Fiber-Reinforced Polymer Reinforcement Ratio on Axial-Flexural Strength of Reinforced Concrete Columns," *ACI Structural Journal*, V. 115, No. 4, July 2018, pp. 1049-1061. doi: 10.14359/51701279
- 10. Khorramian, K., and Sadeghian, P., "Experimental and Analytical Behavior of Short Concrete Columns Reinforced with GFRP Bars under Eccentric Loading," *Engineering Structures*, V. 151, 2017, pp. 761-773. doi: 10.1016/j.engstruct.2017.08.064
- 11. ACI Committee 440, "Building Code Requirements for Structural Concrete Reinforced with Glass Fiber-Reinforced Polymer (GFRP) Bars (ACI CODE-440.11-22) and Commentary," American Concrete Institute, Farmington Hills, MI, 266 pp.
- 12. ASTM D7957/D7957M-22, "Standard Specifications for Solid Round Glass Fiber Reinforced Polymer Bars for Concrete Reinforcement," ASTM International, West Conshohocken, PA, 2022, 5 pp.
- 13. MNL-17(21), ACI Reinforced Concrete Design Handbook, A Companion to ACI 318-19, American Concrete Institute, Farmington Hills, MI, 2019, 568 pp.
- 14. ACI Committee 318, "Building Code Requirements for Structural Concrete (ACI 318-19) and Commentary (ACI 318R-19) (Reapproved 2022)," American Concrete Institute, Farmington Hills MI, 2019, 624 pp.
- 15. Wight, J. K., and Macgregor, J. G., *Reinforced Concrete Mechanics and Design*, sixth edition, Pearson Education, Inc., Upper Saddle River, NJ. 2019.

# Ciassoom

# Integrate (aci) into your classroom!

To support future leaders, ACI has launched several initiatives to engage students in the Institute's activities and programs – select programs that may be of interest to Educators are:

- Free student membership encourage students to sign up
- Special student discounts on ACI 318
   Building Code Requirements for Structural
   Concrete, ACI 530 Building Code Requirements and Specification for Masonry
   Structure, & Formwork for Concrete manual.
- Access to Concrete International free to all ACI student members
- Access to ACI Structural Journal and ACI Materials Journal – free to all ACI student members
- Free sustainability resources free copies of Sustainable Concrete Guides provided to universities for use in the classroom
- Student competitions participate in ACI's written and/or team-based competitions

- Scholarships and fellowships students who win awards are provided up to \$15,000 and may be offered internships and paid travel to attend ACI's conventions
- ACI Award for University Student Activities receive local and international recognition for your University's participation in concreterelated activities
- Free access to the ACI Collection of Concrete Codes, Specifications, and Practices – in conjunction with ACI's chapters, students are provided free access to the online ACI Collection
- ACI online recorded web sessions and continuing education programs – online learning tools ideal for use as quizzes or in-class study material